International Journal of Microwave and Wireless Technologies

cambridge.org/mrf

A quad-band impedance transformer using two-section stubbed coupled line

Xinhuai Wang, Kejiang Li, Yifan Hou, Wen Wang, Hongyang Xu, Yin Xu and Xiao Wei Shi

National Key Laboratory of Radar Detection and Sensing, Xidian University, Xi'an, China

Research Paper

Cite this article: Wang X, Li K, Hou Y, Wang W, Xu H, Xu Y, Shi XW (2025) A quad-band impedance transformer using two-section stubbed coupled line. *International Journal of Microwave and Wireless Technologies* **17**(7), 1125–1130. https://doi.org/10.1017/S1759078725101815

Received: 24 December 2024
Revised: 3 June 2025
Accepted: 7 June 2025

Keywords
coupled line; impedance transformer; quad-band; two-section

Corresponding author: Xinhuai Wang; Email: xinhuaiwang@xidian.eu.cn

Abstract

Based on the stubbed coupled line for matching a load, we design an impedance transformer matched the load of $Z_L = 100\Omega$, working at four frequencies in this paper. This proposed transformer comprises two sections of coupled line constructed from parallel-coupled transmission lines. Two different types of the proposed transformer are given and analyzed, and we derive carefully about the open-circuit form equations for impedance transformer. We fabricate an impedance transformer to certify the validity of design equations theoretically, and the frequency is measured at 0.7/2.4/3.6/5.3 GHz. The measured results are in good agreement with the simulated results at each frequency.

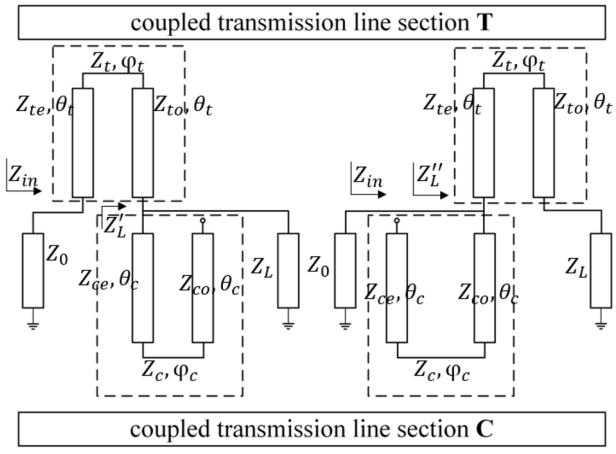
Introduction

An impedance transformer is one of the most important components widely used in radio frequency and microwave fields to match the impedance differences between different circuits or systems to achieve highly efficient signal transmission and maximum power transmission. Impedance transformers can be applied to power divider, couplers, antennas, filters, mixer, power amplifiers, and low noise amplifiers [1–8]. There are many ways to realize multi-band components. A novel approach for designing dual-mode dual-band bandpass filters is proposed in [9]. They realize it by embedding a pair of slits in the square patch, and one transmission zero is introduced between the two passbands. An exact synthesis and design procedure is proposed in [10], which gives a class of wideband dual-band bandpass filters that can achieve both controllable in-band ripple factor and isolation between the dual passband. A mixed transmission zero embedded dual-band impedance transformer that operates at two uncorrelated frequencies in Chuang et al. [11] is presented. By deploying the cross-shaped structure, an impedance transformer that can significantly eliminate the line width limitation of traditional quarter-wave impedance transformer is proposed in Zhu et al. [12]. A novel design of ultra-wideband impedance transformers and power dividers with filtering capabilities is given in Cao et al. [13]. A design of an impedance transformer with wideband, maximally flat real-to-real impedance matching is proposed in Darraji et al. [14], with exact solutions for transmission lines' parameters being derived in explicit form for any impedance transformation ratio being given.

With the development of complexity and miniaturization of device functions, the demand for components that meet the use of multiple frequency bands is increasing. A three-section transmission line transformer is proposed in Jones [15], which can match real impedance at three arbitrary frequencies between assigned frequency f_0 and its third harmonic. Then, a compact quad-frequency impedance transformer with a two-section coupled line is proposed in Schiek and Kohler [16], which can achieve an ideal impedance matching at four frequencies. To match a load at three arbitrary frequencies, a compact tri-band impedance transformer by utilizing stubbed coupled line is proposed in Chongcheawchamnan et al. [17].

A novel type of transformer to match real impedance load at four frequencies is proposed in this paper. The transformer is composed of two sections of stubbed coupled line. We changed the short-circuit form in Chongcheawchamnan et al. [17] into an open-circuit form to reduce the number of grounding holes and simplify the structure of impedance transformer, so the loss of manufacture could be reduced. In this paper, we derive and analyze the design equations carefully. In addition, we also deduce the range of frequency ratios analytically and numerically. We evaluated several cases to certify it is feasible and valid to realize impedance matching theoretically at four different frequencies. We choose the transformer's working frequencies at 0.7/2.4/3.6/5.3 GHz to verify the validity of the proposed impedance transformer in the application. After fabricating and measuring, it turns out that the simulated results are in good agreement with the measured results.

© The Author(s), 2025. Published by Cambridge University Press in association with The European Microwave Association.



(a) type I: stub at the load (b) type II: stub at the source

Figure 1. Structure of the proposed quad-band transformer. (a) Type I: stub at the load. (b) Type II: stub at the source.

Structure and design

Figure 1 shows that the circuit structure of the proposed quad-band impedance transformer is simply composed of two sections of coupled line sections T and C, and section C is an open-circuit form. Section T is the coupled transmission line, and section C is the stubbed coupled line, respectively, in Figure 1(a) and Figure 1(b). The structures of two types are shown in Figure 1(a) and Figure 1(b).

As shown in Figure 1, the odd and even mode characteristic impedances of T and C coupled transmission lines are Z_{to}, Z_{te}, Z_{co}, and Z_{ce} and the image impedance of T and C are Z_t, Z_c. The φ_t and φ_c are insert phases of the coupled transmission line sections T and C. With the equal electrical lengths θ_t and θ_c of the two modes, the odd and even modes, it is set to the same odd and even mode impedance ratio ρ $(\rho > 1)$ for transmission lines according to Jones' theory in Bai et al. [18], so we can give the following equations:

$$Z_t = \sqrt{Z_{te} \cdot Z_{to}} \tag{1}$$

$$Z_c = \sqrt{Z_{ce} \cdot Z_{co}} \tag{2}$$

$$\frac{Z_{te}}{Z_{to}} = \frac{Z_{ce}}{Z_{co}} = \rho \tag{3}$$

$$\cos\varphi_t = \frac{\rho - \tan^2\theta_t}{\rho + \tan^2\theta_t} \tag{4}$$

$$\cos\varphi_c = \frac{\rho - \tan^2\theta_c}{\rho + \tan^2\theta_c} \tag{5}$$

The ratio parameter of the impedance transformer between source impedance and load impedance is defined as follows.

$$K = \frac{Z_0}{Z_L} = \frac{Z_{in}}{Z_L} \tag{6}$$

Type I: coupled line shunted at the load

We can give the input impedance Z_{in} of the two-section line according to the transmission line theory, as in the circuit structure shown in Figure 1(a).

$$Z_{in} = Z_t \frac{Z_L' + jZ_t \tan\varphi_t}{Z_t + jZ_L' \tan\varphi_t} \tag{7}$$

$$Z_L' = \frac{\frac{Z_c}{j\tan\varphi_c} \cdot Z_L}{\frac{Z_c}{j\tan\varphi_c} + Z_L} \tag{8}$$

Substitute (8) into (7) and observe the real part and the imaginary part, respectively, we can get the following equations:

$$\begin{cases} Z_{in}Z_tZ_c = Z_tZ_cZ_L - Z_t^2Z_L\tan\varphi_c\tan\varphi_t \\ jZ_{in}Z_tZ_L\tan\varphi_c + jZ_{in}Z_cZ_L\tan\varphi_t = jZ_t^2Z_c\tan\varphi_t \end{cases} \tag{9}$$

Equation (9) can be written as follows:

$$\begin{cases} \tan\varphi_c\tan\varphi_t = \frac{Z_cZ_L - Z_{in}Z_c}{Z_tZ_L} \\ \frac{\tan\varphi_c}{\tan\varphi_t} = \frac{Z_t^2Z_c - Z_{in}Z_cZ_L}{Z_{in}Z_tZ_L} \end{cases} \tag{10}$$

Then, to simply the derivation process, let $\theta_t = \theta_c = \theta$, therefore $\varphi_t = \varphi_c = \varphi$, and we can rewrite (9) in the following form:

$$\begin{cases} \tan^2\varphi = \frac{Z_cZ_L - Z_{in}Z_c}{Z_tZ_L} \\ 1 = \frac{Z_t^2Z_c - Z_{in}Z_cZ_L}{Z_{in}Z_tZ_L} \end{cases} \tag{11}$$

Let $\alpha \equiv \tan^2\varphi$. By solving (11), the following equation is derived:

$$\begin{cases} Z_t = \sqrt{Z_{in}Z_L - \frac{Z_{in}(Z_{in} - Z_L)}{\alpha}} \\ Z_c = \frac{\alpha Z_tZ_L}{Z_L - Z_{in}} \end{cases} \tag{12}$$

Together with (4), (5), and (11), we can obtain:

$$\begin{cases} \alpha = \tan^2\varphi \\ \tan^2\theta = \rho\frac{1-\cos\varphi}{1+\cos\varphi} = \rho\tan^2\frac{\varphi}{2} \end{cases} \tag{13}$$

We can obtain an expression about θ by solving the equations above.

$$\theta = m\pi \pm \arctan\left(\sqrt{\rho}\tan\frac{n\pi \pm \arctan\sqrt{\alpha}}{2}\right) \tag{14}$$

Both m and n are arbitrary integers, so we can get four unrelated solutions for θ from (14). Since $\theta > 0$ and a small size impedance transformer is what we want to realize. Therefore, $(+)$ sign is chosen in (14) when $m = n = 0$ and $(-)$ sign is chosen in (14) when $m = n = 1$. Considering the generality, we assume that $f_1 < f_2 < f_3 < f_4$, and we can obtain the four fundamental solutions about θ from (14).

$$\begin{cases} \theta_1 = \arctan(\sqrt{\rho}\tan\frac{\arctan\sqrt{\alpha}}{2}) \\ \theta_2 = \arctan(\sqrt{\rho}\tan\frac{\pi - \arctan\sqrt{\alpha}}{2}) \\ \theta_3 = \pi - \arctan(\sqrt{\rho}\tan\frac{\pi - \arctan\sqrt{\alpha}}{2}) \\ \theta_4 = \pi - \arctan(\sqrt{\rho}\tan\frac{\arctan\sqrt{\alpha}}{2}) \end{cases} \tag{15}$$

This means the impedance transformer can perfectly match impedance at four different frequencies. Furthermore, assuming $0 < \theta_1 < \theta_2 < \theta_3 < \theta_4 < \pi$. The relationships between θ_1, θ_2

https://doi.org/10.1017/S1759078725101815 Published online by Cambridge University Press

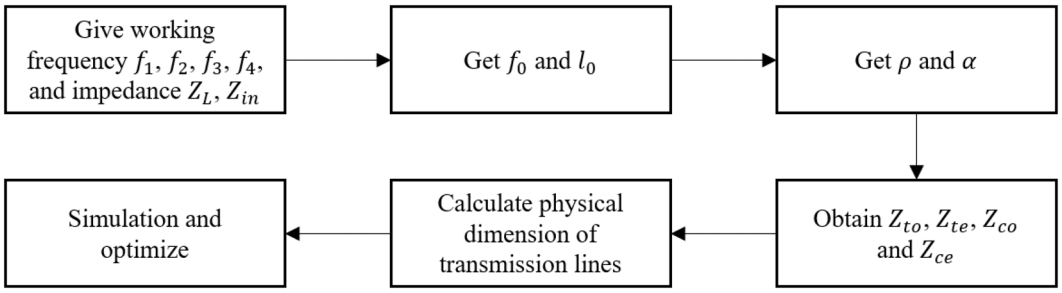


Figure 2. Design process.

θ_3 and θ_4 could be obtained from (15) as follows:

$$\tan\theta_1 \tan\theta_2 = \sqrt{\rho}\tan\frac{\arctan\sqrt{\alpha}}{2}\sqrt{\rho}\tan\frac{\pi-\arctan\sqrt{\alpha}}{2} = \rho \tag{16}$$

$$\frac{\tan\theta_1}{\tan\theta_2} = \tan^2\left(\frac{\arctan\sqrt{\alpha}}{2}\right) \tag{17}$$

$$\theta_1 + \theta_4 = \theta_2 + \theta_3 = \pi \tag{18}$$

According to the electrical length definition, we know

$$\theta = \beta l = \frac{2\pi f}{c} l \tag{19}$$

The l is the physical length of the single coupled line, and the c is the velocity of light. If we fix the physical length of the single coupled line and determine it as l_0, we will obtain

$$\theta_i = \beta_i l_0 = \frac{2\pi f_i}{c} l_0 \quad (i = 1, 2, 3, 4) \tag{20}$$

A frequency variable f_0 can be given from (18) and (20) as follows:

$$f_0 \equiv \frac{f_1+f_4}{2} = \frac{f_2+f_3}{2} = \frac{c}{4l_0} \tag{21}$$

If frequencies f_1, f_2, f_3 are given, the physical length of a single coupled line section l_0 can be calculated from (21) and we can write it as follows:

$$l_0 = \frac{c}{4f_0} \tag{22}$$

Electrical lengths θ_i, ρ, and α can be calculated by

$$\theta_i = \beta_i l_0 = \frac{\pi f_i}{2f_0} \tag{23}$$

$$\rho = \tan\left(\frac{\pi f_1}{2f_0}\right)\tan\left(\frac{\pi f_2}{2f_0}\right) \tag{24}$$

$$\alpha = \tan^2\left(2\arctan\sqrt{\frac{\tan\left(\frac{\pi f_1}{2f_0}\right)}{\tan\left(\frac{\pi f_2}{2f_0}\right)}}\right) \tag{25}$$

So far, the deduction of the design equations for the designed impedance transformer of type I has been completed.

Design process is shown in Figure 2. If we give f_1, f_2, f_3 and f_4 firstly, f_0 and l_0 can be calculated by (21) and (22). Second, ρ and α can be calculated by (24) and (25). Third, we can know the image impedance Z_t and Z_c from (12). Then, according to (1), (2) and (3), the odd and even mode characteristic impedance Z_{to}, Z_{te}, Z_{co}, and Z_{ce} can be obtained. Eventually, the basic parameters of the Quad-band impedance transformer can be determined.

Type II: coupled line shunted at the source

As type II shown in Figure 1(b), with the stubbed coupled line section shunted at the source, the equations can be derived similarly. According to the transmission line theory, we can also give the input Impedance Z_{in} of two-section line.

$$Z_{in} = \frac{\frac{Z_c}{j\tan\varphi_c}Z_L''}{\frac{Z_c}{j\tan\varphi_c}+Z_L''} \tag{26}$$

$$Z_L'' = Z_t\frac{Z_L + jZ_t\tan\varphi_t}{Z_t + jZ_L\tan\varphi_t} \tag{27}$$

Similarly, the solutions are obtained by solving the equations as follows:

$$\begin{cases} Z_t = \sqrt{Z_{in}Z_L - \frac{Z_L(Z_L-Z_{in})}{\alpha}} \\ Z_c = \frac{\alpha Z_t Z_{in}}{Z_{in}-Z_L} \end{cases} \tag{28}$$

These two structures mirror each other, and the design process is the same as described in the case that the stubbed coupled line section C is shunted at the load end. To match real impedance load, it can be seen that in (12) that Z_0 should be smaller than Z_L, however in (28), Z_0 should be larger than Z_L, which means that cases change with structures changing.

Analysis and simulations

The solutions mentioned above are elementary in nature and are in open-circuit form. However, not all frequencies are ideal for realizing the application, so we must consider the available ranges of frequency ratios. Thus, to describe the relationship between different frequencies better, we let $f_2 = pf_1, f_3 = qf_2$,so $f_3 = pqf_1$, where p, q is the frequency-ratio and $1 < p < pq$. So we can rewrite (24) as follows by replacing frequencies.

$$\rho = \tan\frac{\pi}{p(q+1)}\tan\frac{p\pi}{p(q+1)} \tag{29}$$

Then, we obtain by (29) since $\rho > 1$.

$$\frac{\sin\frac{\pi}{p(q+1)}\sin\frac{p\pi}{p(q+1)}}{\cos\frac{\pi}{p(q+1)}\cos\frac{p\pi}{p(q+1)}} > 1 \tag{30}$$

We can get $\cos\frac{\pi}{p(q+1)} > 0$ and $\cos\frac{p\pi}{p(q+1)} > 0$ since $1 < p < pq$. Equation (30) can be derived as follows after rearrangement and

https://doi.org/10.1017/S1759078725101815 Published online by Cambridge University Press

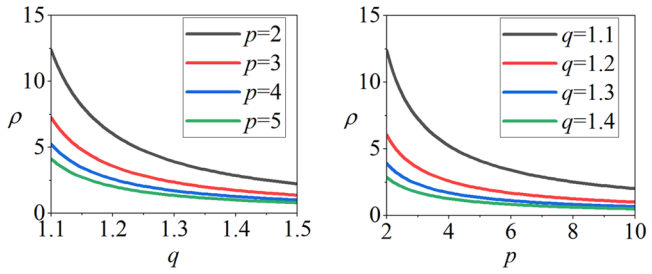


Figure 3. Relationship between ρ, frequency-ratios p and q.

Table 1. Simulations on condition $K = 0.5$ ($p = 2.5$ or $q = 1.5$)

	f_1(GHz)	f_2(GHz)	f_3(GHz)	f_4(GHz)	p	q	ρ
Case1	0.8	2	3	4.2	2.5	1.5	1.69
Case2	0.8	2	3.5	4.7	2.5	1.75	1.08
Case3	1	3	4.5	6.5	3	1.5	1.37
Case4	1.5	3	4.5	6	2	1.5	2.24

using trigonometric formula.

$$\cos\frac{(p+1)\pi}{p(q+1)} < 0 \tag{31}$$

The solution of Equation (31) is

$$\frac{2-p(4n+1)}{p(4n+3)} < q < \frac{2+p(1-4n)}{p(4n+1)} \tag{32}$$

Where n is an arbitrary integer. With $1 < p < pq$, (32) can be simplified as

$$1 < q < \frac{2+p}{p} \tag{33}$$

Multiply by pf_1, we obtain

$$f_1 < f_2 < f_3 < 2f_1 + f_2 \tag{34}$$

Figure 3 shows the relationships between the impedance ratio ρ and frequency ratio p and q, we can obtain this conclusion that ratio ρ is reducing with the increase of p and q, which means ratio ρ is reducing with the increase of designed frequency ratio.

We give some examples under the condition that $K = 0.5$, as listed in Table 1. Figure 4 shows the theoretic $|S_{11}|$ under the condition with fixed f_1, f_2 and $p = 2.5$ and fixed f_2, f_3 and $q = 1.5$. It can be seen that the $|S_{11}|$ is well-matched with designed frequencies.

Experiment results

Considering non-TEM behavior in microstrip realization in the application, a stepped impedance coupled line is used in model building [19].To verify the matching at the four frequency points, we choose F4BM-2 ($tan\delta \leqslant 0.0007$) with a relative permittivity of 2.55 and the thickness h of 0.762mm as the dielectric substrate to fabricate a quad-band impedance transformer at 0.7/2.4/3.6/5.3 GHz, which could be applied to Power Divider, Coupler, Antenna, Filter, Mixer Power Amplifier, and LNA. Here we set $Z_0 = 50\Omega$ and $Z_L = 100\Omega$. The model of the designed impedance transformer with the dimension being labeled and the photo of it are shown in Figure 5 and Figure 6. The numerical results are calculated by MATLAB R2022b, and we obtain the simulated results by Advanced Design Systems (ADS).

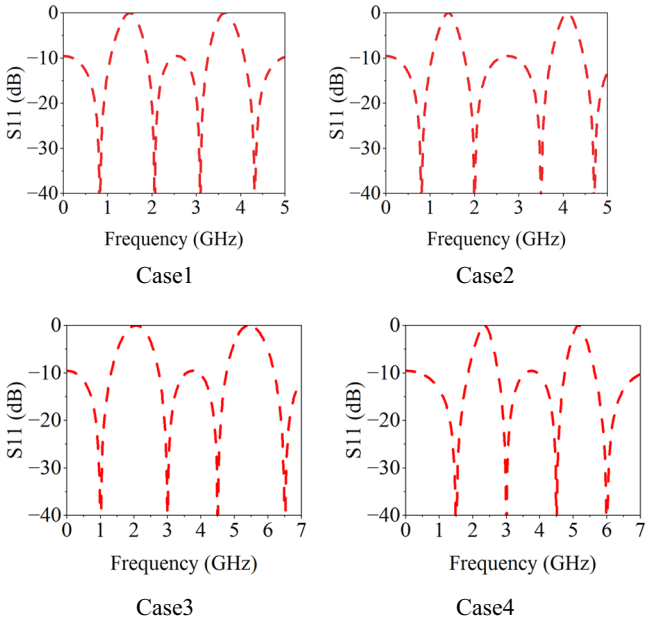


Figure 4. Theoretic $|S_{11}|$ under the conditions from Table 1.

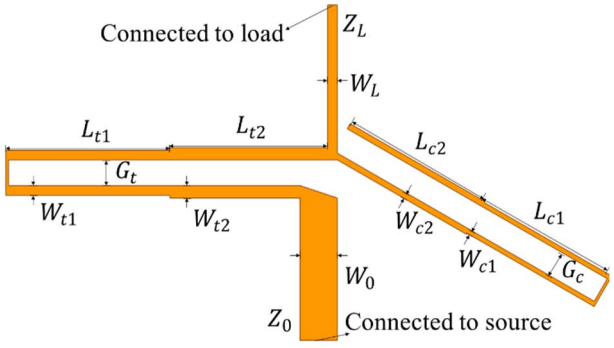


Figure 5. The model of the designed impedance transformer with the dimension being labeled.

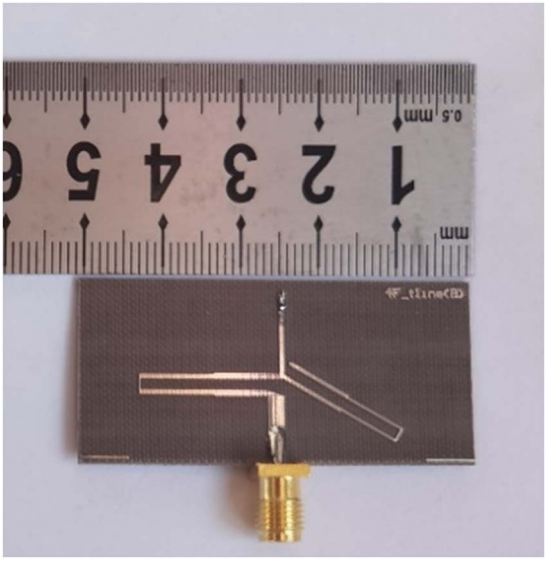


Figure 6. The photo of the designed impedance transformer.

https://doi.org/10.1017/S1759078725101815 Published online by Cambridge University Press

Table 2. Optimized dimensions (unit millimeter)

W_0	W_L	W_{t1}	W_{t2}	W_{c1}	W_{c2}	L_{t1}	L_{t2}	G_t	G_c	L_{c1}	L_{c2}
2.12	0.56	0.55	0.71	0.27	0.46	9.36	8.36	1.45	1.45	7.85	8.40

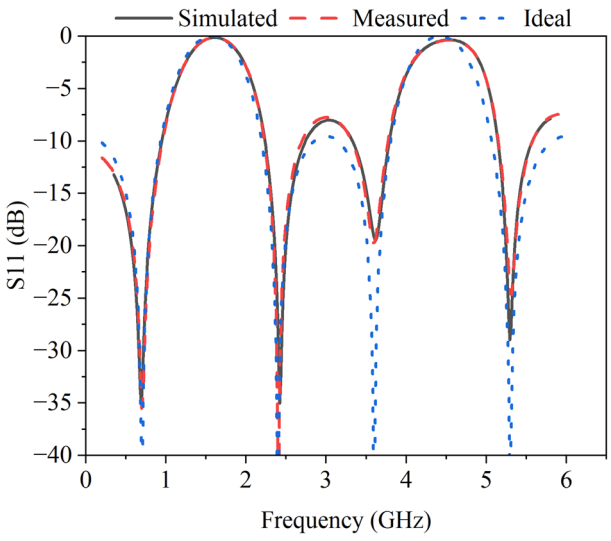


Figure 7. Simulated and measured $|S_{11}|$ results of the designed impedance transformer.

By the equations above, we can calculate that $Z_{te} = 102.19\Omega$, $Z_{to} = 86.50\Omega$, $Z_{ce} = 133.09\Omega$, $Z_{co} = 112.66\Omega$. Then, we optimize the result through simulation and final dimensions are listed in Table 2. It is shown in Figure 7 about the measured results of S-parameters for the magnitude of $|S_{11}|$ obtained from the Agilent N5230A network analyzer and the simulated results. We can directly see that the measured results of the $|S_{11}|$ are about −35.5 dB at 0.7 GHz, −35.8 dB at 2.4 GHz, −19.7 dB at 3.6 GHz, and −24.5 dB at 5.3 GHz. The two curves fit very well in Figure 7, which means that the measured results are in good agreement with the simulated results at four designed frequencies. The designed impedance is practicable. Compared with the result in Chongcheawchamnan et al. [17], simulated and measured curves fit better in this paper. There are some small differences between measured and simulated results, these could be caused by material purity, manufacturing limitation, coaxial line connector welding, and measurement accuracy.

Conclusion

In this paper, we propose a novel quad-band impedance transformer. The proposed impedance transformer can match a real impedance load at four frequencies by using a stubbed coupled line and reduce the impedance transformer's size. Firstly, we give and analyze two types of structures of the proposed impedance transformer and derive design equations logically, which validates the feasibility of the design theoretically. Then, considering the available ranges of frequency ratios, we derive them numerically and several cases are listed and evaluated to prove the feasibility of the application of the designed impedance transformer. The costs of manufacture could be reduced by reducing the grounding holes. Finally, a quad-band transformer working at 0.7/2.4/3.6/5.3 GHz is manufactured and measured to verify the consistency between simulation and application. Considering non-TEM behavior in microstrip realization in the application, a stepped impedance coupled line is used in model building to overcome it. It turns out that the measured results are in good agreement with the simulated results.

Acknowledgement. This work was supported by the Key Research and Development Program of Shaanxi Province under Grant 2020ZDXM5-01.

Competing interests. The authors report no conflict of interest.

References

1. **Roshani S, Dehghani K and Roshani S**. (2019) A Lowpass Filter Design Using Curved and Fountain Shaped Resonators. *Frequenz* **73**(7-8), 267–272. https://doi.org/10.1515/freq-2019-0013.
2. **Bavandpour SK, Roshani S, Pirasteh A, Roshani S and Seyedi H** A compact lowpass - dual bandpass diplexer with high output ports isolation *AEU - International Journal of Electronics and Communications* **135** 2021 https://doi.org/10.1016/j.aeue.2021.153748
3. **Saeedeh L, Saeed R and Sobhan R**, Design of a miniaturized planar microstrip Wilkinson power divider with harmonic cancellation, *Turkish Journal of Electrical Engineering & Computer Sciences*, Vol. 28, 3126–3136, No. 6, 2020.
4. **Cheng F, Du C-H, Wu L and Gu C**. (2024) Compact and ultra-wideband high-efficiency rectifier using asymmetric coupled-line impedance transformer. *International Journal of Microwave and Wireless Technologies* **16**(6), 966–971. https://doi.org/10.1017/S1759078724000813.
5. **Lee JY, Zhu M, Yang K, Lee YC and Idrus II**, Wide-Slot Tri-Band Patch Antenna Fed by Quarter Wave Transformer for Biomedical Applications, IEEE MTT-S International Microwave Biomedical Conference, 232–235, May 2022.
6. **Park JS and Wang H** (2016) A Fully Differential Ultra-Compact Broadband Transformer-Based Wilkinson Power Divider. *IEEE Microwave and Wireless Components Letters* **26**, 255–257. https://doi.org/10.1109/LMWC.2016.2537793
7. **Alsakka MH, Zewani M and Albadawieh A**. (2024) Dual UWB bandpass filter with highly band-to-band rejection using stepped impedance stub-loaded resonators for WBAN health-care applications. *International Journal of Microwave and Wireless Technologies* **16**(3), 409–417. https://doi.org/10.1017/S1759078723001101.
8. **Wong YC, Arslan T and Erdogan AT**, Reconfigurable wideband RF impedance transformer integrated with an antenna for multi-band wireless devices, Loughborough Antennas & Propagation Conference, 1–5, Nov., 2012.
9. **Sung Y** (2010) Dual-Mode Dual-Band Filter With Band Notch Structures. *IEEE Microwave and Wireless Components Letters* **20**, 73–75. https://doi.org/10.1109/LMWC.2009.2038434
10. **Zhang R and Zhu L** (2013) Synthesis and Design of Wideband Dual-Band Bandpass Filters With Controllable In-Band Ripple Factor and Dual-Band Isolation. *IEEE Transactions on Microwave Theory & Techniques* **61**, 1820–1828. https://doi.org/10.1109/TMTT.2013.2256145
11. **Chuang M-L, Wu M-T, Tsai M and Chang C-Y** (2022) Mixed Dual-Band Impedance Transformer With Embedded Transmission Zero. *IEEE Transactions on Circuits and Systems–II: Express Briefs* **69**, 2717–2721. https://doi.org/10.1109/TCSII.2022.3148794
12. **Zhu H-X, Cheong P, Ho K, Tam K-W and Choi -W-W** (2020) Realization of Extremely High and Low Impedance Transforming Ratios Using Cross-Shaped Impedance Transformer. *IEEE Transactions on Circuits and Systems–II: Express Briefs* **67**, 1189–1193. https://doi.org/10.1109/TCSII.2019.2935499

https://doi.org/10.1017/S1759078725101815 Published online by Cambridge University Press

13. **Cao Z, Liu Y, Liang C and Majid I** (2023) Design of UWB Filtering Impedance Transformers and Power Dividers Using Stepped-Impedance Resonators. *Electronics* **12**, 2800. https://doi.org/10.3390/electronics12132800
14. **Darraji R, Honari MM, Mirzavand R, Ghannouchi FM and Mousavi P** (2016) Wideband Two-Section Impedance Transformer With Flat Real-to-Real Impedance Matching. *IEEE Microwave and Wireless Components Letters* **26**, 313–315. https://doi.org/10.1109/LMWC.2016.2548997
15. **Chongcheawchamnan M, Patisang S, Srisathit S, Phromloungsri R and Bunnjaweht S** (2005) Analysis and design of a three-section transmission-line transformer. *IEEE Transactions on Microwave Theory & Techniques* **53**, 2458–2462. https://doi.org/10.1109/TMTT.2005.850408
16. **Bai Y-F, Wang X-H, Gao C-J, Huang Q-L and Shi X-W** (2012) Design of Compact Quad-Frequency Impedance Transformer Using Two-Section Coupled Line. *IEEE Transactions on Microwave Theory & Techniques* **60**, 2417–2423. https://doi.org/10.1109/TMTT.2012.2202682
17. **Wang XH, Zhang L, Xu Y, Bai YF, Liu C and Shi X-W** (2013) A Tri-Band Impedance Transformer Using Stubbed Coupling Line. *Progress in Electromagnetics Research-pier* **141**, 33–45. Jul. https://doi.org/10.2528/PIER13042907.
18. **Jones EMT** (1956) Coupled-Strip-Transmission-Line Filters and Directional Couplers. *IRE Transactions on Microwave Theory and Techniques* **4**, 75–81. https://doi.org/10.1109/TMTT.1956.1125022
19. **Schiek B and Kohler J** (1977) A Method for Broad-Band Matching of Microstrip Differential Phase Shifters. *IEEE Transactions on Microwave Theory & Techniques* **25**, 666–671. https://doi.org/10.1109/TMTT.1977.1129183



Xinhuai Wang received the B.E. degree in electronic science and technology and Ph.D. degree in radio physics from Xidian University, Xi'an, China, in 2004 and 2010, respectively. Since 2010, he has been with the National Key Laboratory of Antennas and Microwave Technology, Xidian University, as a Lecturer. He has been an Associate Professor with Xidian University since 2014. He is currently a Professor and Doctoral Supervisor since 2020. His recent research interests are mainly in microwave circuits and smart antenna system design.



Kejiang Li was born in Chengdu, Sichuan, CHN in 1998. He received the B.E. degree in electronic information engineering from Xidian University, Xi'an, China, in 2022. He is pursuing a master's degree in electronic and information from Xidian University. His recent research interests include flexible antenna, millimeter wave radar, and impedance transformer.



Yifan Hou was born in Hanzhong, Shaanxi, CHN in 2000. He received the B.E degree in electronic engineering from Xidian University, Xi'an, China, in 2022. He is pursuing a master's degree in electronic and information from Xidian University. His recent research interests include RF circuits and systems, microwave device simulation and design, as well as smart antenna design.



Wen Wang was born in Xi'an, Shaanxi, CHN in 1998. He received the B.E degree from Northwestern Polytechnical University, Xi'an, China.in 2018, and the M.E degree from Nanjing Research Institute of Electronics Technology, Nanjing, China, in 2021. He is currently pursuing thePh.D. degree in electronic science and technology from Xidian University, Xian, China. His current research interests include wearable, antenna, and radio frequency technologies and applications.



Hongyang Xu was born in Jining, Shandong, CHN in 1997. He received the B.E. degree from Qingdao Agricultural University, Qingdao, China in 2020, and the M.E. degree in New Generation Electronic Information Technology from Xidian University, Xi'an, China in 2023. His current research includes microwave and radio frequency (RF) technology, millimeter wave radar signal processing, and embedded systems development.



Yin Xu received the B.E., M.E., and Ph.D. degrees from Xidian University, Xi'an, China, in 2006, 2009, and 2013, respectively. She is working at Xidian University as an Associate Professor. Her recent research interests are mainly in the electromagnetic field and microwave technology.



Xiaowei Shi received the B.E., and Ph.D. degrees from Xidian University, Xi'an, China, in 1982 and 1995, respectively. He is engaged in teaching and research in the field of electromagnetic field and microwave technology at the School of Electronic Engineering, Xidian University. His recent research interests include: computational electromagnetics, array antennas, smart antennas, radio frequency identification, and microwave circuits and systems.

https://doi.org/10.1017/S1759078725101815 Published online by Cambridge University Press